THE JOURNAL OF PHYSICAL CHEMISTRY B

Article

SERR-Spectroelectrochemical Study of a *cbb* Oxygen Reductase in a Biomimetic Construct

Smilja Todorovic, Andreia Verissimo, Nattwandee Wisitruangsakul, Ingo Zebger, Peter Hildebrandt, Manuela M. Pereira, Miguel Teixeira, and Daniel H. Murgida

J. Phys. Chem. B, **2008**, 112 (51), 16952-16959 • Publication Date (Web): 24 November 2008

SERR-Spectroelectrochemical Study of a cbb_3 Oxygen Reductase in a Biomimetic Construct

Smilja Todorovic,*,† Andreia Verissimo,† Nattwandee Wisitruangsakul,‡ Ingo Zebger,‡ Peter Hildebrandt,‡ Manuela M. Pereira,† Miguel Teixeira,† and Daniel H. Murgida*,§

Instituto de Tecnologia Química e Biológica, Universidade Nova de Lisboa, EAN, 2780-157 Oeiras, Portugal, Departamento de Química Inorgánica, Analítica y Química Física/INQUIMAE, Facultad de Ciencias Exactas y Naturales, Universidad de Buenos Aires, Ciudad Universitaria, Pab. 2, piso 1, C1428EHA Buenos Aires, Argentina, and Max-Volmer-Laboratorium für Biophysikalische Chemie, Institut für Chemie, Technische Universität Berlin, Sekr. PC14, Strasse des 17. Juni 135, D-10623 Berlin, Germany

Received: September 4, 2008; Revised Manuscript Received: September 29, 2008

The cbb_3 oxygen reductase from *Bradyrhizobium japonicum* was immobilized on nanostructured silver electrodes by anchoring the enzyme via a His-tag to a Ni-NTA coating, followed by reconstitution of a lipid bilayer. The immobilized enzyme retains the native structure and catalytic activity as judged by in situ surface-enhanced vibrational spectroscopy and cyclic voltammetry, respectively. Spectroelectrochemical titrations followed by SERR spectroscopy of the integral enzyme and its monohemic (fixO) and dihemic subunits (fixP), allowed the determination of the reduction potentials for the different heme *c* groups. Both in the isolated subunits and in the integral enzyme the Met/His-coordinated hemes from the two subunits present identical reduction potentials of 180 mV, whereas for the bis-His heme from fixP the value is ca. 400 mV. The determination of reduction potentials of the individual hemes *c* reported in this work provides the basis for further exploring the mechanism of electroprotonic energy transduction of this complex enzyme.

Introduction

Heme-copper oxygen reductases are terminal respiratory chain complexes that catalyze reduction of molecular oxygen to water in aerobic prokaryotes and mitochondria.[1] The catalytic reaction is coupled to translocation of protons across the membrane, creating a difference in the transmembrane electrochemical potential that drives ATP synthesis and other potential-dependent processes.[2,3]

Oxygen reductases of cbb_3 type, which are expressed in various bacteria under microaerobic conditions, exhibit several unique characteristics.[4] Phylogenetically, they are the most distant and the least understood members of the heme-copper oxygen reductase superfamily.[2,4,5] In contrast to type A and B enzymes, cbb_3 oxygen reductases lack the Cu_A electron entry site[1] and the highly conserved tyrosine residue covalently bound to the histidyl Cu_B ligand, whose function is exerted by another tyrosine present in the helix VII of cbb_3.[4,6] Moreover, based on amino acid sequence alignment, it has been shown that many of the amino acid residues involved in proton conduction through the D- and K-channels of A-type enzymes are also absent in cbb_3 oxygen reductases.[2,4−6] Interestingly, the expression of cbb_3 from *Rhodobacter sphaeroides* has been shown to sensitively respond to changes in oxygen partial pressure.[7−10] Another peculiarity of cbb_3 enzymes is that they exhibit the highest NO reductase activity among the members of the superfamily.[5,11]

Clearly, in sharp contrast to mitochondrial-like heme-copper oxygen reductases, understanding of the functioning of cbb_3 enzymes is still an elusive goal. On the basis of the characteristics described above, one might anticipate differences in terms of regulation of electron flow and proton translocation mechanisms.[3,12−14]

The *Bradyrhizobium japonicum* cbb_3 enzyme (*Bj* cbb_3) studied in the present work is a type C oxygen reductase that contains three major subunits: a membrane integral subunit I (fixN), which houses a low-spin heme *b* and the catalytic center (heme b_3 - Cu_B), and subunits II (fixO) and III (fixP), containing one and two hemes *c*, respectively. The cbb_3 encoding operon also includes a gene that codes for a fourth small membrane subunit (fixQ), which is typically lost during purification.[5]

In a recent study the redox potentials of the detergent-solubilized integral enzyme from *B. japonicum* have been determined by redox titrations monitored by UV−visble specroscopy.[15] The assignment of the observed redox transitions to individual centers, however, is not complete as the method employed is not able to distinguish hemes of the same *c*-type. Here we report the titration of the heme *c*-containing individual subunits (fixO and fixP) by surface-enhanced resonance Raman (SERR) spectroelectrochemistry, as well as of the catalytically active integral *B. japonicum* enzyme immobilized and embedded into a biomimetic membrane. The results allow for an unambiguous assignment of the redox potentials of the individual hemes *c* as a prerequisite for understanding the functioning of this complex enzyme.

Materials and Methods

Bacterial Strains and Growth Conditions. *B. japonicum* strain Bj4639, containing the pRJ4639 plasmid which has the genes coding for the $FixN^{His}OQP$ operon of the cbb_3 oxygen reductase,[16] was grown in a 30 L reactor at 28 °C, 150 rpm and low aeration (oxygen tensions below 1%) during 5 days. In these conditions the $FixN^{His}OQP$ operon was induced and the cbb_3 oxygen reductase expression enhanced. *Escherichia coli* BL21DE gold strains were cloned with the pEC86 plasmid containing the *ccm*ABCDEFGH genes needed for the assembly of *c*-type

* Corresponding authors. E-mail: S.T., smilja@itqb.unl.pt; D.H.M., dhmurgida@qi.fcen.uba.ar.
† Universidade Nova de Lisboa.
‡ Technische Universität Berlin.
§ Universidad de Buenos Aires.

10.1021/jp807862m CCC: $40.75
Published on Web 11/24/2008

hemes. These cells were further transformed with plasmids pRJ4646 and pRJ4591,[17] containing the *fixO* and *fixP genes*, respectively. Cells for the expression of fixO and fixP subunits were grown at 30 °C in LB media at 150 rpm, and gene expression was induced at a cell density of $A_{600} = 0.3$ with 0.4% arabinose during 18 h at 15 °C in both cases.

Protein Purification. The *Bj* cbb_3 oxygen reductase was purified from the membranes according to the previously described protocol.[15,16] *E. coli* cells, grown for the expression of the fixO and fixP subunits, were harvested and ruptured in a French press. Both soluble fractions were obtained by ultracentrifugation at 138000 *g*. All chromatographic steps were done on Pharmacia Hi Load or LKB HPLC systems at 4 °C. The soluble proteins were loaded on a Q-Sepharose Fast Flow column equilibrated with 20 mM Tris−HCl buffer pH 7.5 (5 °C), 1 mM PMSF, and eluted with a linear gradient of NaCl. Fractions containing the overexpressed *c*-type cytochromes were eluted at approximately 100 mM NaCl. After concentration the fractions containing the fixO and fixP subunits were loaded on a Ceramic Hydroxyapatite column, previously equilibrated with 20 mM phosphate buffer pH 7.5, 1 mM PMSF. Cytochrome *c*-containing fractions were eluted before application of the linear gradient of 20−1000 mM phosphate buffer. After subsequent concentration, both fractions were injected into a Sephadex G-50 column, equilibrated and eluted with 20 mM Tris−HCl buffer pH 7.5, 1 mM PMSF, 150 mM NaCl. Both proteins were pure after this gel filtration step as judged by SDS-PAGE and UV−visible spectroscopy. The purified fixO and fixP have apparent molecular masses of 27 kDa. The absorption spectra of both, as purified and dithionite reduced recombinant proteins are similar and present Soret and α bands maxima characteristic of *c*-type cytochromes. Heme content in recombinant proteins, indicated the presence of one and two hemes in fixO and fixP, respectively.

Resonance Raman (RR) Spectroscopy. All measurements were performed with a confocal microscope coupled to a single stage spectrograph (Jobin Yvon XY-800) equipped with 1800 L/mm grating and liquid-nitrogen-cooled back-illuminated CCD detector. Samples were placed in a quartz rotating cell and excited with the 413 nm line from a krypton ion laser (Coherent Innova 302). RR spectra of 15 μM fixP and 20 μM fixO (20 mM Tris−HCl, 0.01% DM pH 8) oxidized (as purified) and sodium dithionite reduced states, were measured with a laser power of 0.5 mW and accumulation times of 30 s. Due to extreme sensitivity toward photoreduction, RR spectra of 10 μM integral oxidized cbb_3 oxygen reductase were measured with a laser power of 0.12 mW and accumulation times of 8 s. The fully reduced enzyme was measured after addition of sodium dithionite. All RR solution spectra reported here represent an average of 10 to 20 spectra.

Surface-enhanced Resonance Raman (SERR) Experiments. Ag disks electrodes were polished and roughened following published procedures[18] and coated with biocompatible films for subsequent protein immobilization. For fixO and fixP the Ag disks were coated with mixed self-assembled monolayers of pentanethiol and 6-mercapto-1-hexanol by overnight incubation in a 1:1 (1 mM / 1 mM) ethanolic solution of the thiols. Integral cbb_3 was immobilized via its His-tag, according to the protocol described earlier,[19] or on a detergent (DM) coated electrode.[20] The coated Ag disks, which served as working electrodes, were placed at the bottom of a homemade rotating electrochemical cell equipped with a Ag/AgCl reference electrode and a Pt counter electrode. A detailed description of the electrochemical cell is given elsewhere.[18,21] The cell potential was controlled by a PAR 263-A potentiostat. SERR spectra were collected in backscattering geometry using the confocal Raman microscope described above. All measurements were performed with 413-nm excitation. The spectra of fixO and fixP were obtained with a long working distance objective (20×, N.A. 0.35), 1 mW laser power and 30s accumulation. SERR spectra of the integral enzyme were recorded with an immersion objective (100×, N.A. 1.00), 90 μW laser power and 10 s accumulations. Typically, over 10 spectra were collected and averaged.

All experiments were done under anaerobic conditions in the closed electrochemical cell, in the presence of the glucose/glucose oxidase/catalase system for oxygen removal and applying argon overpressure above the protein solution. Spectroelectrochemical SERR titrations were performed in the −400 to +340 mV range, with 20−50 mV steps. At each potential, the system was allowed to equilibrate for 5 min, as found to be sufficient for reaching the equilibrium state at each electrode potential, irrespectively of the protein or the immobilization procedure. All potentials cited in this work refer to the NHE.

Surface-Enhanced Infrared Absorption (SEIRA) Spectroscopy. SEIRA measurements were performed in Kretschmann-ATR configuration using a semicylindrical shaped silicone (Si) crystal (20 × 25 × 10 mm of W × L × H) under an incident angle of 60°. Thin gold (Au) films were formed on the flat surface of the Si substrate by electroless deposition.[22] Spectra were recorded from 4000 to 1000 cm^{-1} at a spectral resolution of 4 cm^{-1} on a Bruker IFS66v/s spectrometer equipped with a photoconductive MCT detector. Depending on the particular experiment, between 138 and 2760 scans were coadded for a spectrum.

The protein was injected into the buffer solution (20 mM Tris−HCl, pH 8, 0.01% DM) to yield a final concentration of 2 μM. A reference spectrum of the buffer was measured in the absence of the protein. All steps of cbb_3 binding to Ni-NTA and subsequent embedding of cbb_3 into lipid membrane reconstitution on an Au electrode were followed by SEIRA difference spectroscopy. The equilibrium state of the immobilized cbb_3 was reached after about 2 h. Spectra of cbb_3 adsorbed on the bare Au electrode and via His-tag immobilization were collected at open-circuit potential.

For electrochemical measurements a three electrode setup was used including an Au-film working electrode (1.54 cm^2 exposure area) in combination with a Pt and saturated Ag/AgCl electrodes, mounted in one compartment cylindrical cell. Electrode potentials were controlled by an Autolab PGSTAT 12 potentiostat.

Cyclic Voltammetry (CV). CV measurements were performed in the SEIRA electrochemical cell described above. After lipid reconstitution around the immobilized cbb_3, as described below, KCl was added to the buffer solution to achieve a final concentration of 50 mM. Subsequently, voltammograms were measured in the absence and presence of the artificial electron donor *N,N,N′,N′*-tetramethyl-*p*-phenylenediamine (TMPD) and the natural substrate (O_2). The electrode potentials were swept from 0 to 550 mV at variable rates.

Results and Discussion

FixO and fixP Subunits. The individual fixO and fixP subunits, overexpressed in *E. coli* with their transmembrane domain truncated, were first characterized by RR spectroscopy in solution using Soret band excitation. RR spectroscopy is a powerful tool for studying structure, dynamics and reaction mechanisms of heme proteins.[18,23−25] In the high frequency region (ca. 1300−1700 cm^{-1}), RR spectra contain a number of

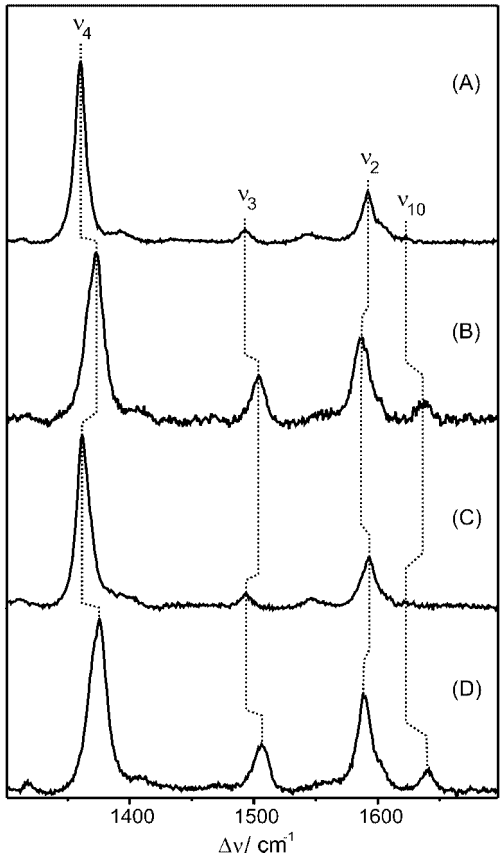

Figure 1. RR spectra in solution of (A) reduced fixO, (B) oxidized fixO, (C) reduced fixP, and (D) oxidized fixP. All measurements were done with 413 nm excitation, 1 mW laser power at sample and 30 s accumulation time.

bands which are sensitive indicators of the heme type, redox state, coordination pattern and spin of the heme iron. The spectra of fixO and fixP, both in the fully oxidized (as purified) and in dithionite reduced forms, bear remarkable similarities in the low and high frequency regions (Figure 1).

Ferric and ferrous forms of the monohemic fixO subunit display RR spectra characteristic of a six-coordinated low spin (6cLS) heme *c* with methionine and histidine as axial ligands, i.e., similar to cytochrome *c*.[25,26] In the reduced form the high frequency region could be simulated with the Lorentzian marker bands ν_4 (1360 cm^{-1}), ν_3 (1493 cm^{-1}), ν_2 (1592 cm^{-1}), and ν_{10} (1624 cm^{-1}). For oxidized fixO the marker bands shift to higher frequencies as expected and, except for a minor contribution of ferrous protein, the spectrum can be satisfactorily simulated with the set of marker bands ν_4 (1373 cm^{-1}), ν_3 (1504 cm^{-1}), ν_2 (1587 cm^{-1}), and ν_{10} (1637 cm^{-1}) which is indicative of a single *c*-type heme with Met/His axial coordination pattern.

At first sight, the RR spectra of ferrous and ferric fixP subunit are very similar to those of subunit fixO, except for small shifts, broadening and asymmetry of some bands. Specifically, we note that for ferrous fixP the ν_4-envelope requires a minimum of two Lorentzian bands at 1360 and 1365 cm^{-1} for simulation (Figure 2). Similarly, two bands at 1370 and 1376 cm^{-1} are required to simulate the ν_4-envelope of ferric fixP suggesting the presence of two different hemes. Also, the simulation of the ν_3-envelope of oxidized fixP requires a minimum of two bands at 1504 and 1509 cm^{-1}. The spectral region at ca. 1600 cm^{-1} is more difficult to simulate due to the superposition of a larger number of bands, but also here we note an upshift of the ν_2-band of fixP with respect to fixO.

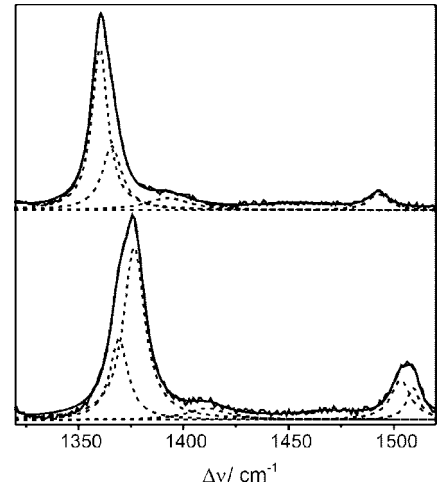

Figure 2. RR spectra of the ferrous (top) and ferric (bottom) fixP subunit including the component spectra for the ν_3 and ν_4 bands in dotted lines. Experimental conditions as given in Figure 1.

These findings indicate the presence of two type-*c* heme groups with different coordination patterns in fixP. One of the spectral components is closely related to the one observed for monohemic fixO subunit, which is in turn similar to mitochondrial cytochrome *c*, whereas the other component exhibits an upshift that resembles the imidazole complex of horse heart cytochrome *c*.[26,27]

Therefore, the spectral analysis of purified fixP subunit is consistent with two 6cLS type-*c* hemes with Met/His and His/His coordination. On the other hand, there are no spectral indications for other coordination patterns indicative for a partially unfolded protein (e.g., high-spin species) neither in fixO nor in fixP samples, as also confirmed by UV−vis and EPR spectra (data not shown).

The redox behavior of both subunits was investigated by SERR spectroelectrochemistry. This technique allows for the potentiometric titration of species adsorbed on a nanostructured metal electrode surface while simultaneously probing structural properties of the adsorbate. A key issue, however, is the immobilization of the protein on the metal surface under conditions that preserve its native structure. To that end, a number of methodologies applicable to soluble and membrane proteins have been developed, mainly based on self-assembled monolayers (SAMs) of functionalized mercaptanes.[19,22,23] For immobilization of fixO and fixP, mixed SAMs of 1:1 pentanethiol/6-mercapto-1-hexanol (mol/mol) ensure an efficient protein adsorption as judged from the intense SERR signals (Figure 3).[28] Adsorption could be detected neither on the pure methyl-terminated nor on the pure hydroxyl-terminated SAMs, revealing the interplay of hydrophobic and polar interactions as crucial for protein binding.

SERR spectra of fixO and fixP recorded at sufficiently negative potentials are essentially identical to the corresponding RR spectra of the dithionite reduced samples in solution, indicating that no structural changes have occurred on the level of the heme group(s) upon immobilization. For both subunits, different results are obtained upon electrochemical oxidation as shown for fixO in Figure 3. At potentials higher than 190 mV, we note considerable intensity at ca. 1493 cm^{-1}, which cannot solely be due to the ν_3 mode of the reduced form because its strongest band at ca. 1360 cm^{-1} (ν_4) is detectable only as a shoulder of the strong 1370 cm^{-1} signal of the ferric hemes. Conversely, the ν_3 mode for ferric 5cHS hemes is typically observed also at ca. 1490 cm^{-1}. Thus we conclude that, in

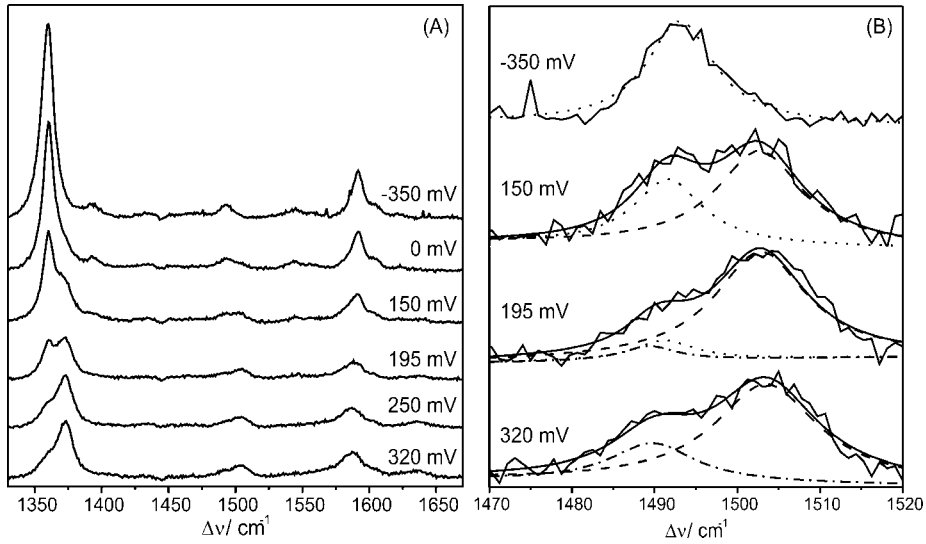

Figure 3. Potential-dependent SERR spectra of fixO subunit immobilized on electrodes coated with mixed monolayer (1:1 C_6 CH_3/OH). Panel B displays the ν_3 region including the fitted component spectra of the ferrous 6cLS (dotted line), ferric 6cLS (dashed line) and ferric 5cHS (dashed-dotted) states. Measurements were performed at 413 nm excitation, 1 mW laser power at sample and accumulation times of 30 s.

addition to the native 6cLS species identified in RR spectra of the proteins in solution, SERR spectra contain small but detectable contributions of another oxidized species in which one ligand is dissociated from the heme iron and thus adopts a 5cHS configuration. In analogy to observations for other *c*-type heme proteins immobilized on electrodes, we attribute this species to a fraction of the His/Met ligated hemes in which the Fe-Met bond is broken.[18,24] Similar spectral changes were observed for fixP at high electrode potentials and, thus, attributed to the loss of the Met ligand for a fraction of the His/Met hemes.

SERR spectroelectrochemical titrations of the immobilized fixO and fixP were carried out in the range from −400 to +350 mV. Because the spectral parameters of the 5cHS species are unknown a reliable component analysis of the spectra based on multiple bands is not feasible. Therefore, quantitative spectral analysis was limited to the strongest band, ν_4, which is also the most sensitive indicator of the redox state. At each potential the ν_4 envelope was fitted with Lorentzian bands with variable positions and widths to determine the potential-dependent contributions of ferrous (ca. 1360 cm^{-1}) and ferric hemes (ca. 1373 cm^{-1}). At potentials below +195 mV, all spectra could be consistently analyzed on the basis of four (two ferric and two ferrous) and two (one ferric and one ferrous) bands for fixP and fixO, respectively. For analysis of the SERR spectra recorded at more positive potentials one additional band was necessary to account for the ferric 5cHS species (vide supra).[29] Determination of reduction potentials was based on total intensities of ferrous and ferric species, i.e., the sum of bands at ca. 1360 and 1370 cm^{-1}, respectively. This procedure was adopted because it is less sensitive to uncertainties in the determination of spectral parameters for the 5 identified species in the case of fixP, or 10 or more for the integral protein (see below). The potential-dependence of the coadded spectral contributions of the ferrous hemes (I_{red}) can be expressed by eq 1, where the intensity at the most negative potential (fully reduced sample) is arbitrarily defined as 1.

$$I_{red} = \sum_{i=1}^{n} \frac{1}{1 + \exp\left[-\frac{zF}{RT}(E - E_i^0)\right]} \qquad (1)$$

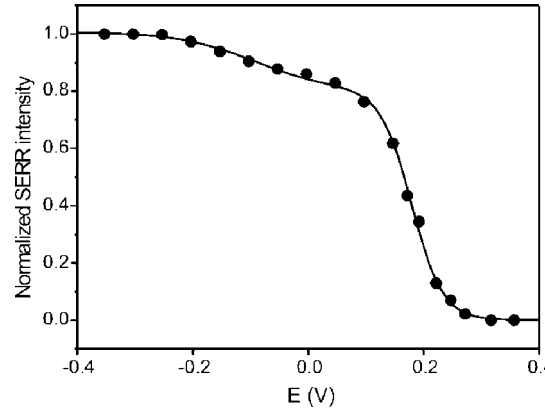

Figure 4. SERR titration of fixO, immobilized on electrodes coated with mixed monolayers, with two redox transitions, $E^\circ = -120$ mV; $z = 0.62$ and $E^\circ = 180$ mV; $z = 0.95$. Data points correspond to the normalized intensity of the ν_4-band using the spectrum recorded at the most negative potential as a reference. The curve represents the best fit of eq 1 to the experimental data for $n = 2$ and using E° and z as adjustable variables.

where E is the electrode potential, n is the number of transitions, E_i^0 is the reduction potential for an individual transition corresponding to the exchange of z electrons, and F, R and T have the usual meanings.

Figure 4 shows the normalized intensity of the ferrous spectral contribution for fixO as a function of the poised electrode potential and the best fit of eq 1 to the experimental data.

The analysis reveals a sharp transition with a potential $E^\circ =$ 180 mV and a number of transferred electrons very close to one ($z = 0.95$), which accounts for ca. 80% of the total SERR signal. The determined E° value falls within the range expected for a Met/His-coordinated type-*c* heme protein.[5] A minor fraction of the immobilized fixO, i.e., the remaining 20% of the total SERR signal, undergoes a rather broad redox transition at ca. −120 mV. The broadness of this transition ($z = 0.62$) suggests a distribution of protein structures possessing different reduction potentials, such that the determined E° value represents an average of the ensemble. The broad distribution, as well as the negative value of the average E° are consistent with a minor fraction of adsorbed fixO that is partially unfolded. Note that full oxidation of the heme is achieved at ca. 300 mV.

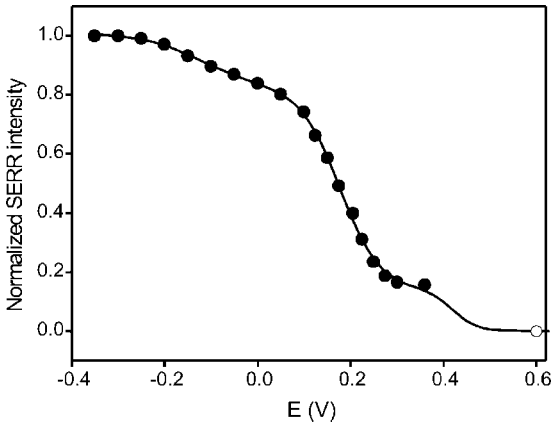

Figure 5. SERR titration of fixP, immobilized on electrodes coated with mixed monolayers, with 3 redox transitions: $E° = -120$ mV, $z = 0.40$; $E° = 180$ mV, $z = 0.80$ and $E° \sim 400$ mV. Data points correspond to the normalized intensity of the ν_4-band using the spectrum recorded at the most negative potential as a reference. The curve represents the best fit of equation 1 to the experimental data for $n = 2$ and using $E°$ and z as adjustable variables. For the high potential transition, given the lack of data points, we fixed $z = 1$ and forced the system to converge to $I = 0$ at high potentials by inserting an artificial data point at $E = 0.6$ V (open circle).

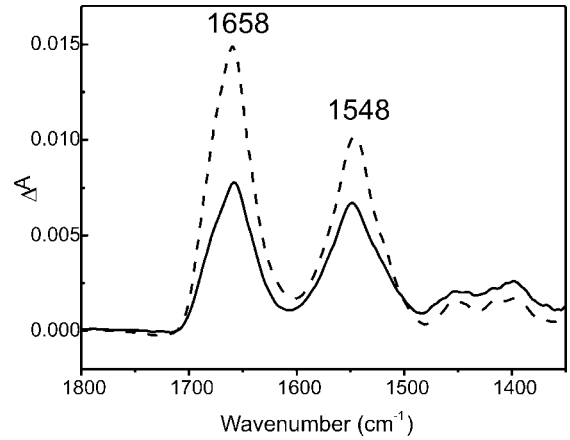

Figure 6. Absolute SEIRA spectra of integral *B. japonicum* cbb_3 oxygen reductase immobilized on detergent coated electrode (solid line) and via His-tag/Ni-NTA (dotted line).

The quantitative analysis of the potential-dependent SERR spectra of fixP immobilized on identical biomimetic electrodes yields a picture that is very similar to fixO (Figure 5) displaying a sharp transition at 180 mV ($z = 0.80$) and a broad one at ca. -120 mV ($z = 0.40$).

However, in contrast to fixO, the SERR intensity of ferrous fixP is still significant at the highest potentials that can be achieved with the Ag working electrode, thus indicating the existence of a third redox transition beyond the accessible potential window. As shown in Figure 5, a simulation of the third transition points out to a lower limit of ca. 400 mV for the corresponding midpoint potential. Like for fixO, the most negative and broad transition is ascribed to partially unfolded protein.

Integral cbb_3 Oxygen Reductase. Membrane bound redox proteins are integrated into the lipid bilayer, thus exerting their function in a hydrophobic environment, under restricted motion and defined directionality, in the presence of a transmembrane potential.[28] Thus, for the immobilization of integral *B. japonicum* cbb_3 on silver electrodes and subsequent SERR spectroelectrochemical titration, we have chosen a strategy that mimics the physiological environment as closely as possible. The metal surface was coated with a 3,3′-dithiobis[*N*-(5amino-5-carboxypentyl)propionamide-*N*,*N*′-diacetic acide] dihydrochloride (NTA) and incubated in a $NiCl_2$ solution to form a Ni-NTA monolayer. Subsequently, the modified electrode was incubated in a solution containing integral cbb_3 solubilized with *n*-dodecyl-β-D-maltoside. The engineered enzyme contains a histidine-tag on the C-terminus of subunit I, i.e., on the cytoplasmic side under in vivo conditions, which serves as an anchor to the Ni-NTA coated electrode. The last immobilization step consists of the reconstitution of a lipid bilayer by addition of 1,2-diphytanoyl-*sn*-glycero-3-phosphocholine and removal of the solubilizing detergent with biobeads.[19,21] Thus, in the final construct the integral cbb_3 is attached to the electrode surface via the His-tag and embedded within a lipid bilayer that mimics the basic features of a natural membrane. Each immobilization step was monitored by SEIRA spectroscopy. As shown in Figure 6, SEIRA spectra of the immobilized protein are dominated by the amide I and II modes at 1658 and 1548 cm^{-1}, respectively, which are sensitive to the protein secondary structure. For the Ni-NTA immobilization procedure stable protein signals were obtained after 2 h of incubation (Figure 6, dotted line). For a protein with a high content of preferentially parallel helices, such as the 12 trans-membrane ones in the subunit I of cbb_3,[5,30,31] SEIRA spectra are sensitive to the orientation of the helices with respect to the electrode surface, which is reflected in the intensity ratio of amide I and amide II bands. The amide I mode is mainly composed by the C═O stretching modes of the peptide bonds. In the SEIRA spectrum of cbb_3 it is observed at 1658 cm^{-1} (Figure 6), a characteristic position for a largely α-helical peptide. Because this mode is associated with dipole moment changes parallel to the axis of the helices, a preferential enhancement of the absorption band occurs when the helices are oriented perpendicular to the surface. Conversely, the dipole moment changes of the amide II mode (1548 cm^{-1}) which is mainly composed of N−H in-plane bending and C−N stretching coordinates, are perpendicular to the helix axis and thus will gain a weaker enhancement for helices oriented in an upright position.[32] Consequently, one expects a relatively high amide I/amide II intensity ratio for the His-tag-immobilized cbb_3 in which the transmembrane helices should largely adopt perpendicular orientation with respect to the electrode surface. A more random orientation of the enzyme is obtained upon unspecific adsorption of the solubilized cbb_3 on a detergent-coated electrode.[20] This is reflected by a ca. 2 times more intense amide I band and a 1.5 times higher amide I/amide II intensity ratio for the His-tag bound cbb_3 (Figure 6, dashed line) than for the enzyme adsorbed on detergent coated Au surface (Figure 6, solid line). Therefore, we can conclude that the cbb_3 is largely uniformly oriented when immobilized via His-tag/Ni-NTA. Upon addition of excess of imidazol to the solution SERR spectra vanish, indicating specific binding of the protein His-tag to the Ni-NTA monolayer.[33]

The oxygen reductase catalytic activity of the immobilized cbb_3 was controlled *in situ* by cyclic voltammetry. As shown in Figure 7, large electrocatalytic currents are observed under aerobic conditions in the presence of the artificial electron donor *N*,*N*,*N*′,*N*′-tetramethyl-p-phenylendiamine (TMPD), whereas only capacitive currents are observed in the absence of TMPD (Figure 7).[33,34]

RR spectra of the dithionite-reduced cbb_3 in solution are characterized by relatively broad bands due to the spectral overlapping of the five heme groups, and are very similar to the RR spectra of cbb_3 isolated from *P. stutzeri* and *R.*

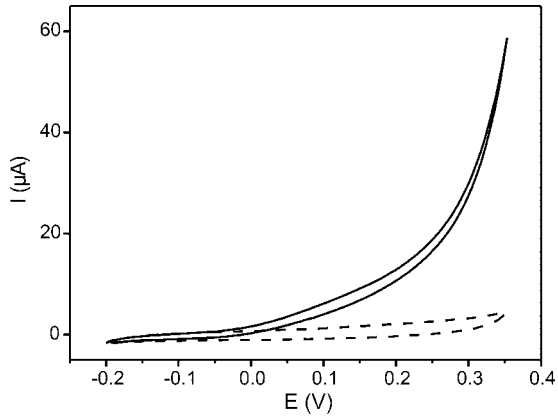

Figure 7. Cyclic voltammetry (CV) of membrane-reconstituted integral cbb_3 immobilized via the His-tag/Ni-NTA strategy. Solid line: CV in the presence of the artificial electron donor TMPD and O_2. Dashed line: CV in the absence of TMPD.

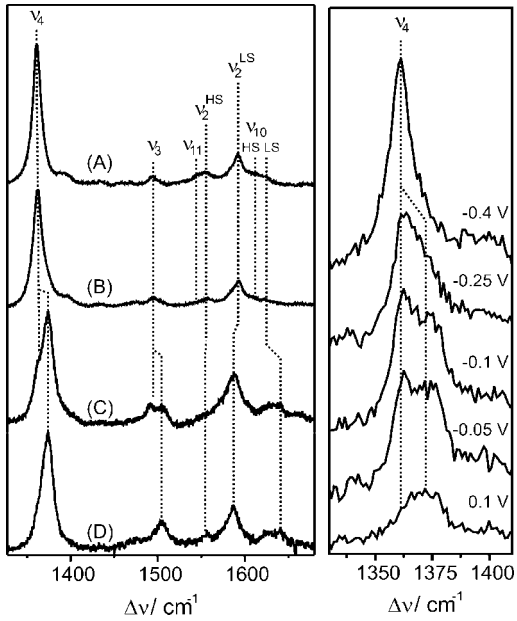

Figure 8. Left panel: RR (A and D) and SERR (B and C) spectra of integral cbb_3 in solution and adsorbed on a detergent-coated electrode, respectively. (A) dithionite and (B) electrochemically (−300 mV) reduced protein; (C) electrochemically oxidized (+350mV) and (D) as purified protein. Right panel: the ν_4 region of SERR spectra of His-tag/Ni-NTA immobilized cbb_3 recorded at different potentials in the presence of redox mediators.

spherodides[35,36] (Figure 8A) with the marker bands ν_4 (1360 cm^{-1}), ν_3 (1494 cm^{-1}), ν_2 (1558 cm^{-1} for the HS heme *b* and 1591 cm^{-1} for LS hemes *b, c*), ν_{11} (1540 cm^{-1}) and ν_{10} (1610 cm^{-1} for HS heme *b* and 1625 cm^{-1} for LS hemes *b, c*). SERR spectra of specifically (Ag/Ni-NTA/His-tag constructs) and nonspecifically (detergent-mediated adsorption) immobilized cbb_3 recorded at sufficiently negative electrode potentials are essentially identical to the RR spectra of the dithionite-reduced enzyme in solution (Figure 8), although the signal-to-noise ratio in the first case is significantly poorer due to the large separation of the heme groups from the Ag surface in this biomimetic construct.

Thus, it can be safely concluded that the native structure of the integral protein is largely preserved upon immobilization, at least for the fully reduced form, which is in agreement with the catalytic activity observed by CV. Furthermore, SERR spectra respond sensitively and in a reproducible manner to changes in the poised potential in both directions, demonstrating reversible oxidation and reduction of the immobilized enzyme. However, at least for the enzyme directly adsorbed on the detergent-coated electrode, we note an increase of a 5cHS contribution in the ferric form which adds to that of the ferric b_3 species (Figure 8). This conclusion is derived from the increased intensity at ca. 1491 cm^{-1}, which cannot be solely attributed to the ν_3 mode of ferrous hemes. Most likely, this extra ferric 5cHS contribution originates from the partial loss of the Met ligands from the fixO and fixP hemes, in analogy to the observations made for the isolated subunits. Conversely, even at the most positive potential that can be applied to the Ag electrode (+350 mV), there is still a residual portion of ferrous heme. These findings indicate an incomplete oxidation of the protein at the most positive potentials that can be achieved at the Ag electrode.[20] The same conclusions also appear to be valid for the His-tag immobilized enzyme although a detailed comparison of the spectra is aggravated by the limited signal-to-noise ratio. The poorer signal-to-noise ratio in this case is due to the significantly longer separation of the heme groups with respect to the SER-active substrate, which was estimated to be ca. 45 Å for a similar CcO-NTA construct,[19] and the fact that the electromagnetic enhancement decays strongly with the distance.[37] In spite of these limitations, the error in the quantification of the ferrous and ferric forms based on the ν_4-band is only about 10%.

Due to this limitation, the analysis of the potential-dependence of ferrous vs. ferric heme contributions to the SERR spectra of cbb_3 in Ag/Ni-NTA/His-tag constructs was limited to the most prominent band ν_4, which is also the most sensitive indicator of the redox state, as described above for the individual subunits. The SERR measurements were performed under anaerobic conditions after careful degassing of the solution and maintaining argon overpressure throughout the experiment. A laser power below 100 μW and constant rotation of the working disk electrode were employed to avoid photoreduction and laser induced damage.[19,21] The experiments were carried out in the presence of a mixture of redox mediators which cover a broad potential range, ca. −450 to +400 mV.[38] A selection of SERR spectra recorded at different electrode potentials is shown in Figure 8.

At each potential the ν_4 envelope was fitted with Lorentzian bands with variable positions and widths to determine the total contributions of ferrous (ca. 1360 cm^{-1}) and ferric hemes (ca. 1373 cm^{-1}). Figure 9 shows the potential dependence of the normalized SERR intensity of the ferrous spectral component obtained with this treatment, where each point represents the average of at least 3 independent determinations. A fit of eq 1 to the experimental data should yield the reduction potentials of the different redox centers in the construct. This procedure, however, is associated with some uncertainty due to the limited data set and the large number of adjustable parameters associated with the five spectrally similar hemes. Nevertheless it is clear that the data can be simulated with a broad transition at ca. −120 mV, one transition with $z = 1$ at ca. 180 mV and one additional transition at potentials higher than ca. 350 mV. Note that these values are identical to those determined for the hemes *c* of the individual subunits fixO and fixP (Table 1). Thus, as for the individual subunits, the first transition is assigned to a fraction of partially unfolded protein (see above). The second transition (180 mV) is assigned to the Met/His coordinated hemes *c* of subunits fixO and fixP which are undistinguishable. Finally, the unresolved high potential transition must include the bis-His-coordinated heme *c* from subunit fixP, as observed

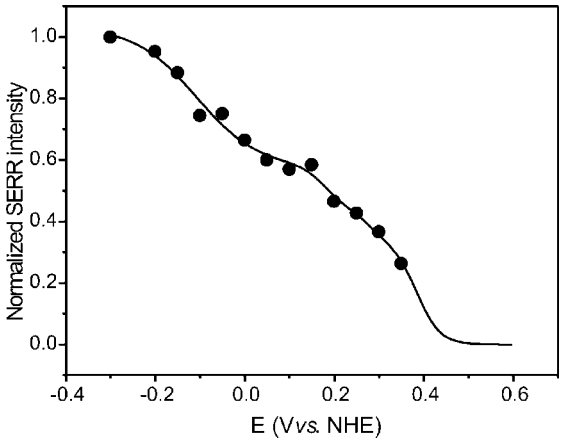

Figure 9. SERR titration of cbb_3 immobilized via His-tag in the presence of redox mediators. Data points correspond to the normalized intensity of the ν_4-band using the spectrum recorded at the most negative potential as a reference. The line is a simulation based on eq 1 taking the parameters obtained for the individual subunits (see text above and Table 1).

TABLE 1: Midpoint Potentials of Integral cbb_3 and the fixO and fixP Subunits As Obtained from SERR Spectroelectrochemical Titrations at pH 8.0

	heme *c* FixP, His/His	heme *c* FixP Met/His	heme *c* FixO Met/His	hemes *b*[a]
fixO			180 ± 10	
fixP	≥400	180 ± 10		
cbb_3-His-tag[b]	≥400	180 ± 10	180 ± 10	280 385
cbb_3 (solution)[a]		190, 290, 395		280 385

[a] Data taken from Verissimo et al. for pH 7.9.[15] [b] Immobilization via Ag/Ni-NTA/His-tag.

for the isolated subunit. According to Verissimo et al. the midpoint potentials for hemes *b* and b_3 at pH ~ 8 are 280 and 385 mV, respectively. These values are compatible with the current results. The solid line in Figure 9 corresponds to a simulation of the data using these two midpoint potentials for hemes *b*, the three values determined for hemes *c* from fixO and fixP subunits, and one negative value for the HS species. The reduction potentials obtained in this way and their assignments are summarized in Table 1, along with data taken from the literature. Note that for the hemes *c* of cbb_3 Verissimo et al. reported three different values (190, 290 and 395 mV), which were not assigned to individual hemes.[15] In the light of the present results it appears reasonable to assign the first two values to the Met/His coordinated hemes *c* and the most positive one to the heme with bisHis coordination. Thus, the only contradiction between the present and previous results refers to the one with the Met/His coordinated hemes *c*. The origin of this discrepancy is not clear, but the present data on the isolated subunits show unambiguously that the two Met/His-coordinated hemes *c* have identical midpoint potentials of ca. 180 mV. Furthermore, we have no indication that these values change in the membrane-reconstituted integral enzyme.

Note that midpoint potentials have been determined on the basis of relative intensities of the ν_4 mode and not on relative concentrations. This approach tacitly assumes that the ratio of the SERR (RR) scattering cross sections for the reduced and oxidized forms is the same for all hemes. This seems to be a reasonable approximation because variations of the cross section ratio by a factor 2 do not cause errors in the redox potential determination by more than 20 mV.

Conclusions

The purified cbb_3 oxygen reductase from *B. japonicum* displays RR spectra very similar to those previously reported for related enzymes from different organisms.[35,36]

The monohemic subunit fixO shows marker bands for a *c*-type heme with a Met/His axial coordination pattern, whereas the subunit fixP possess two different hemes *c* with Met/His and bis-His ligand pairs as the most likely axial coordination ligands. In addition to these spectral features, the integral enzyme displays the characteristic fingerprints of HS and LS hemes *b*.

A prerequisite for understanding the functioning of complex multicenter redox enzymes is the determination of individual potentials and their possible coupling. This task becomes particularly challenging when different redox centers are structurally and spectroscopically similar, as it is the case for the pentahemic cbb_3 oxygen reductase. Indeed, conflicting values of midpoint potentials and experimental errors of their determination larger than 100 mV are not unusual even for much simpler oxygen reductases.[5,15,20] The situation is aggravated by the inherent instability of large membrane complexes and artifacts that can be introduced depending on the solubilizing detergents. Thus, the present comparative spectroelectrochemical analysis of isolated subunits and the integral enzyme in biomimetic constructs substantially facilitates the characterization of the individual cofactors. As shown by in situ SERR spectroscopy and CV, the enzyme retains its structure and catalytic activity in the immobilized state. Furthermore, the spectroelectrochemical response of cbb_3 in the presence of redox mediators is reversible and reproducible. The results indicate that the Met/His coordinated hemes *c* from subunits fixO and fixP exhibit identical midpoint potentials of 180 mV both in the individual subunits and in the integral enzyme, implying that interactions between subunits do not modulate their redox properties. A similar conclusion can be extracted for the bisHis coordinated heme *c* from subunit fixP which also possesses a similar midpoint potential of ca. 400 mV both in the isolated subunit and in the integral enzyme.

The sequence of electron transfer events and their coupling to proton translocation in cbb_3 is far from being elucidated. However, it is reasonable to assume that the Met/His heme *c* of either fixO or fixP subunit which present the lowest redox potentials ($E^\circ = 180$ mV) may serve as the electron entry site of the enzyme. The subsequent electron acceptors may be the bis-His heme *c* in fixP or/and eventually the hemes *b* in the catalytic subunit. On the other hand, it has been reported that fixP is not essential for the catalytic activity of the cbb_3 enzyme from *P. stutzeri*,[5,39,40] implying that electrons can be directly transferred from heme *c* in fixO to heme *b*. Note that, on the basis of the E° values reported here, this latter reaction has a driving force similar to the alternative intra-fixP electron transfer pathway, although the values of ΔG of single steps are clearly not a sufficient criterion for defining electron pathways.

The role of fixP under physiological conditions remains to be clarified. It has been suggested that it might be associated with oxygen sensing properties. Also, it was found that fixP binds carbon monoxide stoichiometrically upon dithionite reduction.[5,17,41,42] A dual function was proposed for the cbb_3 enzyme from the purple photosynthetic bacterium *R. sphaeroides*, as an oxygen reductase and an oxygen sensor. Photosynthesis related genes are turned off under aerobic conditions, with the inhibitory signal being proportional to the electron flow through the cbb_3 oxidase.[7−10]

Further work is necessary to elucidate electron transfer pathways in cbb_3 and, specifically, the role of fixP.

Acknowledgment. This work has been supported by ANPCyT (PICT2006-459; D.H.M.), by the DFG (Cluster of Excellence "Unifying concepts in catalysis"; P.H.), by the FCT (PTDC/QUI/64550/2006, PTDC/BIA-PRO/67263/2006 and POCTI BIA/PRO/58686/2004 to S.T., M.P. and M.T., respectively) and by CRUP-DAAD A-10/07 (S.T. and P.H.). Dr. Hans Martin Fisher is gratefully acknowledged for the kind gift of *B. japonicum* Bj4639 strain. We thank Dr. Ligia M. Saraiva for helping with the expression of the FixO and FixP subunits.

References and Notes

(1) Garcia-Horsman, J. A.; Barquera, B.; Rumbley, J.; Ma, J.; Gennis, R. B. *J. Bacteriol.* **1994**, *176*, 5587–5600.

(2) Pereira, M. M.; Teixeira, M. *Biochim. Biophys. Acta* **2004**, *1655*, 241–247.

(3) Wikstrom, M. *Biochim. Biophys. Acta* **2004**, *1655*, 241–247.

(4) Sharma, V.; Puustinen, A.; Wikstorm, M.; Laakkonen, L. *Biochemistry* **2006**, *45*, 5754–5765.

(5) Pitcher, R. S.; Watmough, N. J. *Biochim. Biophys. Acta* **2004**, *1655*, 388–399.

(6) Hemp, J. C.; Barquera, B.; Gennis, R. B.; Martinez, T. J. *Biochemistry* **2005**, *44*, 10766–10775.

(7) Oh, J.-I.; Kaplan, S. *J. Biol. Chem.* **2002**, *277*, 16220–16228.

(8) Oh, J.-I.; Kaplan, S. *Mol. Microbiol.* **2001**, *39*, 1116–1123.

(9) Myllykallio, H.; Zannoni, D.; Daldal, F. *Proc. Natl. Acad. Sci. U.S.A.* **1999**, *96*, 4348–4353.

(10) Garcia-Horsman, J. A.; Berry, E.; Shapleigh, J. P.; Alben, J. O.; Gennis, R. B. *Biochemistry* **1994**, *33*, 3113–3119.

(11) Forte, E.; Urbani, M.; Saraste, M.; Sarti, P.; Brunori, M.; Giuffre, A. *Eur. J. Biochem.* **2001**, *268*, 6486–6491.

(12) Michel, H. *Biochemistry* **1999**, *38*, 15129–15140.

(13) Artzatbanov, V.; Konstantinov, A.; Skulachev, V. *FEBS Lett.* **1978**, *87*, 180–185.

(14) Rich, P. R. *Aust. J. Plant. Physiol* **1995**, *22*, 479–486.

(15) Verissimo, A.; Sousa, F. L.; Baptista, A. M.; Teixeira, M.; Pereira, M. M. *Biochemistry* **2007**, *46*, 13245–13253.

(16) Arslan, E.; Kannt, A.; Thony-Meyer, L.; Hennecke, H. *FEBS Lett.* **2000**, *470*, 7–10.

(17) Arslan, E.; Schulz, H.; Zufferey, R.; Kunzler, P.; Thony-Meyer, L. *Biochem. Biophys. Res. Commun.* **1998**, *251*, 744–747.

(18) Murgida, D. H.; Hildebrandt, P. *J. Phys. Chem. B* **2001**, *105* (8), 1578–1586.

(19) Friedrich, M. G.; Giess, F.; Naumann, R.; Knoll, W.; Ataka, K.; Heberle, J.; Hrabakova, J.; Murgida, D.; Hildebrandt, P. *Chem. Commun.* **2004**, 2376–2377.

(20) Todorovic, S.; Pereira, M. M.; Bandeiras, T. M.; Teixeira, M.; Hildebrandt, P.; Murgida, D. *J. Am. Chem. Soc.* **2005**, *127*, 13561–13566.

(21) Hrabakova, J.; Ataka, K.; Heberle, J.; Hildebrandt, P.; Murgida, D. *Phys. Chem. Chem. Phys.* **2006**, *8*, 759–766.

(22) Miyake, H.; Ye, S.; Osawa, M. *Electrochem. Commun.* **2002**, *4*, 973–977.

(23) Rivas, L.; Murgida, D.; Hildebrandt, P. *J. Phys. Chem. B* **2002**, *106*, 4823–4830.

(24) Murgida, D. H.; Hildebrandt, P. *J. Am. Chem. Soc.* **2001**, *123* (17), 4062–4068.

(25) Murgida, D. H.; Hildebrandt, P. *Acc. Chem. Res.* **2004**, *37* (11), 854–861.

(26) Hildebrant, P. In *Cytochrome c. A Multidicsiplinary Approach*; Scott, R. A., Mauk, A. G., Eds.; University Science Books: Sausalito, CA: 1996; pp 285−314.

(27) Rivas, L.; Soares, C. M.; Baptista, A. M.; Simaan, A. J.; Di Paolo, R. E.; Murgida, D. H.; Hildebrandt, P. *Biophys. J.* **2005**, *88*, 4188.

(28) Murgida, D.; Hildebrandt, P. *Phys. Chem. Chem. Phys.* **2005**, *7*, 3773–3784.

(29) Dopner, S.; Hildebrandt, P.; Mauk, A. G.; Lenk, H.; Stempfle, W. *Spectrochim. Acta* **1996**, *51*, 573–584.

(30) Zufferey, R.; Thony-Meyer, L.; Hennecke, H. *FEBS Lett.* **1996**, *394*, 349–352.

(31) Zufferey, R.; Arslan, E.; Thony-Meyer, L.; Hennecke, H. *J. Biol. Chem.* **1998**, *273*, 6452–6459.

(32) Marsh, D.; Muller, M.; Schmitt, F.-J. *Biophys. J.* **2000**, *78*, 2499–2510.

(33) Ataka, K.; Giess, F.; Knoll, W.; Naumann, R.; Haber-Pohlmeier, S.; Richter, B.; Heberle, J. *J. Am. Chem. Soc.* **2004**, *126*, 16199–16206.

(34) Pitcher, R. S.; Cheesman, M. R.; Watmough, N. J. *J. Biol. Chem.* **2002**, *277*, 31474–31483.

(35) Varotsis, C.; Babcock, G. T.; Garcia-Horsman, J. A.; Gennis, R. B. *J. Phys. Chem.* **1995**, *99*, 16817–16820.

(36) Pinakoulaki, E.; Stavrakis, S.; Urbani, A.; Varotsis, C. *J. Am. Chem. Soc.* **2002**, *124*, 9378–9379.

(37) Aroca, R. *Surface-Enhanced Vibrational Spectroscopy*; John Wiley & Sons: West Sussex, U.K., 2006.

(38) Hellwig, P.; Ostermeier, C.; Richter, O. M.; Pfitzner, U.; Odenwald, A.; Ludwig, B.; Michel, H.; Mantele, W. *Biochemistry* **1998**, *37*, 7390–7399.

(39) Zufferey, R.; Preisig, O.; Hennecke, H.; Thony-Meyer, L. *J. Biol. Chem.* **1996**, *271* (15), 9114–9119.

(40) de Gier, J.-W. L.; Schepper, M.; Reijnders, W. N. M.; van Dyck, S. J.; Slotboom, D. J.; van Spanning, R. J. M.; van der Oost, J. *Mol. Microbiol.* **1996**, *20*, 1247–1260.

(41) Pitcher, R. S.; Brittain, N. J.; Watmough, N. J. *Biochemistry* **2003**, *42*, 11263–11271.

(42) Wang, J.; Gray, K. A.; Daldal, F.; Rousseau, D. L. *J. Am. Chem. Soc.* **1995**, *117*, 9363–9364.

JP807862M